USING SYNTHETIC APERTURE RADAR DATA DOME COLLECTIONS FOR BUILDING FEATURE ANALYSIS

B Corbett Centre for Electronic Warfare Information and Cyber, Cranfield University, Defence Academy of the United Kingdom, UK

D Andre Centre for Electronic Warfare Information and Cyber, Cranfield University, Defence Academy of the United Kingdom, UK

ABSTRACT

Low-frequency synthetic aperture radar (LF-SAR) is a remote sensing measurement technique that can aid in covert intelligence gathering capabilities for detecting concealed targets in building, and obscured phenomena in general. The Airbus Defence and Space Ltd LF-SAR data dome project has provided a coherently collected three-dimensional data set using airborne circular SAR (CSAR) trajectories, with the potential of providing volumetric SAR imagery of obscured regions inside buildings. Preliminary results of this collection are presented. Both the linear strip-map and CSAR datasets provided contain a great deal of information. Early results show promise, but have revealed the fundamental challenge with low-frequency remote sensing, that being the presence of radio-frequency interference, which reduces the quality of SAR image products.

1 INTRODUCTION

The ability to gather intelligence of concealed areas, buildings etc. is a key interest in modern military intelligence gathering while similar techniques can also have a great impact in a wide variety of civilian applications. Collecting this kind of information through a remote sensing technique allows the measurement process to be completed covertly and from a standoff distance.

Synthetic aperture radar (SAR) is a remote sensing imaging technique, which uses microwave frequency electromagnetic waves, and signal processing to produce high resolution images. It has proven its effectiveness when imaging a variety of landscapes, cities and a variety of specific objects [1], [2]. Another benefit of this imaging technique is that the radar antennas can be mounted on a variety of platforms; airborne, satellite and ground-based systems have all been created, each with their own benefits and drawbacks [2]–[4].

Low-frequency (LF) radio-frequency (RF) applications, e.g. mobile communications, have a well-established history of achieving good performance when penetrating through a variety of building materials [5]–[7]. Hence, utilising this frequency range is the ideal solution for using SAR measurement techniques to image the interior of buildings. Usage of SAR in this manner falls into the recent advances of the sub-field *through-wall LF-SAR*.

The potential for this remote sensing concept will be discussed along with the various issues and difficulties which arise when operating at the desired low-frequencies, not just to the image formation processing but also to the physical data collection as well.

Specifically, the work presented here will contribute towards the larger Remote Intelligence of Building Interiors (RIBI) programme, funded by DSTL.

2 SAR COLLECTION GEOMETRIES

Traditional airborne SAR platforms traverse a linear trajectory and have a side looking antenna angled downwards to image the ground. This is more commonly known as *stripmap* SAR [8, p.381]. However, this type of collection geometry can limit the quality of the SAR image produced in a number of ways.

For example, when a small area is being imaged, a restriction is imposed by the relationship between the size of the synthetic aperture, and the antenna beam width. Restricting the synthetic aperture distance, and reducing the azimuthal angular diversity over the scene, thus limiting the maximum achievable cross-range resolution (δ_{cr}) [1, p.41-49]. The cross-range resolution is approximately as follows,

$$\delta_{cr} = \frac{\lambda_c}{2\theta_a \cos\theta_e} \quad (1)$$

where θ_a is the synthetic aperture angle, θ_e is the elevation angle (both in radians) and λ_c is the centre wavelength of your transmitted pulse [1, p.34-41].

For the maximum synthetic aperture angle possible a circular SAR (CSAR) trajectory is required, see Fig 1 [2], [3, p.486]. This type of data acquisition allows for 360° azimuthal diversity of scene and therefore the best possible cross-range resolution [9].

Therefore, this makes it the ideal collection geometry for imaging a specific target, i.e. a building of interest. This is because the circular acquisition geometry measures all aspect views of the target, allowing the image analyst to select any aspect views from the full data set for analysis. This geometry also allows high cross-range resolution.

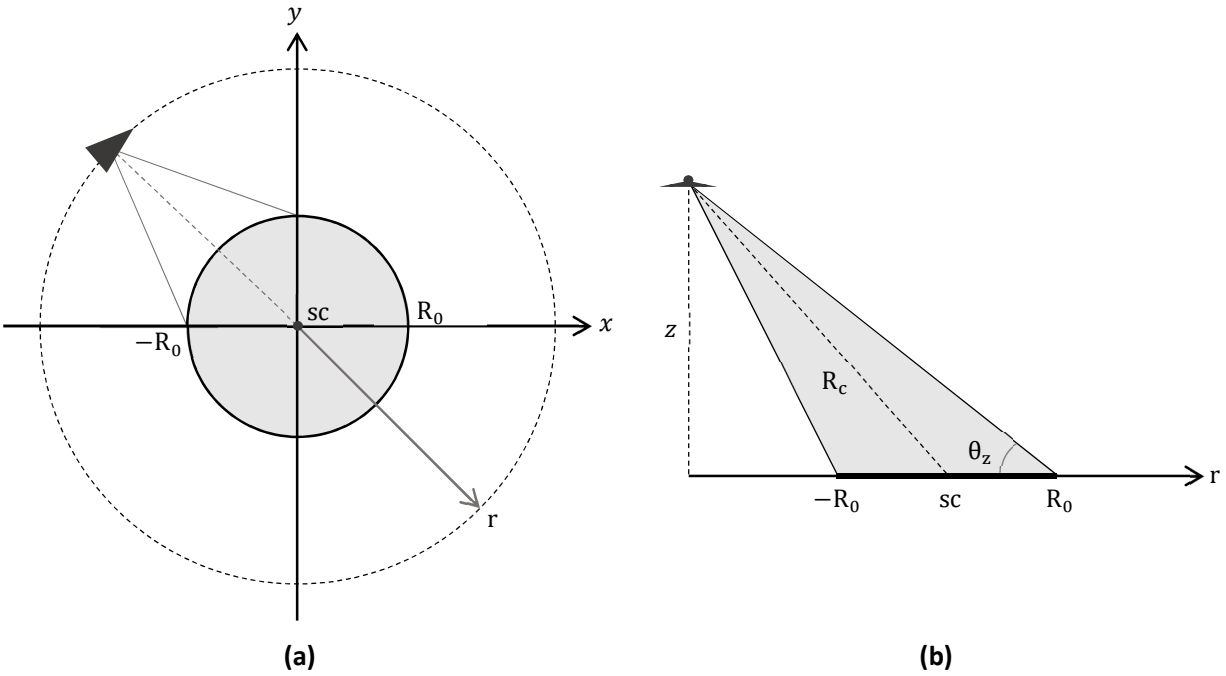

Fig 1. *CSAR collection geometry* [8]. *Where R_0 is half of the beam width ground footprint extent, therefore the radius of the target area illuminated by the radar antenna. R_c is the range to the scene centre (sc) from the platform's location. r is the ground range distance and θ_z is the elevation angle of the platform.*
(a) Top view.
(b) Side view.

3 AIRBUS LF-SAR DATADOME PROJECT

To be able to exploit the most information possible for an imaged scene, repeat measurements are often desired. For example, two measurements of the same scene will allow one to undertake subtractions of the data with the aim of revealing features that have changed between the times when the two scans took place [10]. One difficulty of gathering this kind of measurement data outside of controlled laboratory environment is ensuring that there is coherence between each data acquisition. The Airbus Defence and Space Ltd & DSTL LF data dome project aimed to overcome this.

The LF data dome project was undertaken to produce a large collection of LF-SAR datasets for a variety of targets and location areas in the UK. The datasets for each target area are collected in such a way they can be combined coherently.

The terminology of 'data dome' refers to a 3D collected dataset with measured aspect angles varying in both azimuth and elevation, that when combined coherently produces a hemisphere of data in the 'k-Space' frequency support domain of the target scene, Fig 2 [9].

The result of a data dome collection is that it enables one to produce both tomographic and volumetric SAR images from the same data set, which in turn produces significantly more useable and exploitable information from the same dataset [9]. This increase in the number potentially significant detectable phenomena within the data is of key interest to intelligence services.

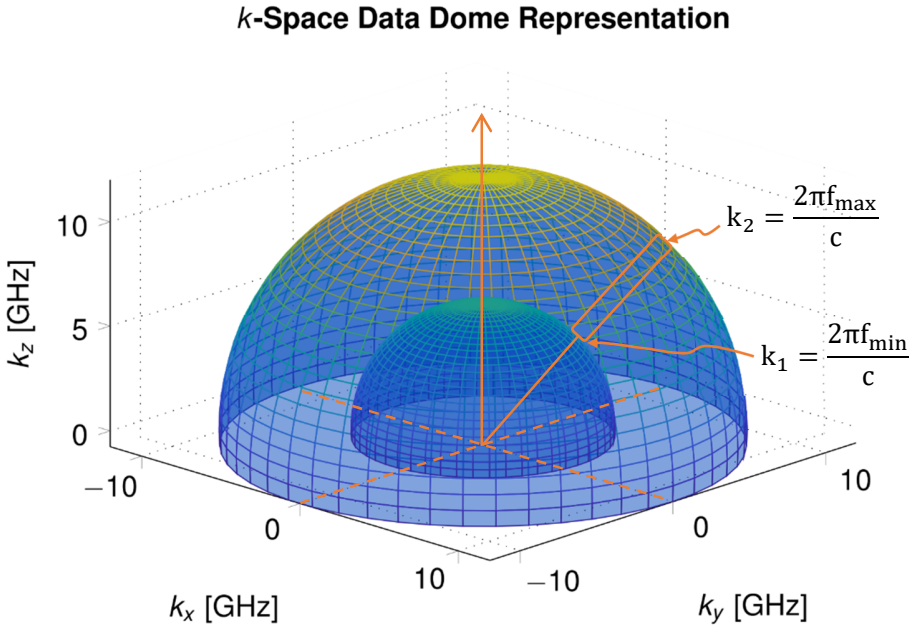

Fig 2. *k-Space data dome visualisation, where k represents a complex wavenumber* [9].

3.1 Bright Sapphire II

The radar sensor used to complete the data dome collections was the Bright-Sapphire II instrument developed and operated by Airbus Defence and Space Ltd. The LF radar sensor operates over the frequency bandwidth of 150-1300MHz and offers quad polarisation operating modes [9].

3.2 LF-SAR Data Collection Trials – Target & Imaged Scene

The dataset provided to the authors by Airbus was obtained over the Country Retreat Lodges holiday site in Mablethorpe, Lincolnshire, Fig 3. The target building in the scene is a single Scandinavian style lodge. The building is constructed predominantly of pine cut at 80mm thick for the walls and pine planks for the roof, which also has a mineral/felt covering.

The target building has five rooms that contain standard household furniture, typical of UK holiday homes. Located within and around the target building several calibration targets were placed, each with their latitude and longitude coordinates recorded. This was done to aid in characterising the data during the image formation and analysis phase. See Fig 4.

Fig 3. *The Sandilands, Arkle Lodge. Located at Country Retreat Lodges holiday site in Mablethorpe, Lincolnshire.*

(a) **(b)**

Fig 4. *Calibration targets located within Arkle Lodge.*
(a) Square Trihedral: Azimuthal angle = 90°, Elevation angle = 14.6°, Height above ground = 1.5m, Latitude = 53.29196°, Longitude = 0.27983°.
(b) Sphere: Height above ground = 0.6m, Latitude = 53.29191°, Longitude = 0.027953°.

3.3 LF-SAR Data Collection Trials – Measurement Details

The target area was measured 32 times over the elevation angle range of ≈20° to ≈70°, Fig 5.

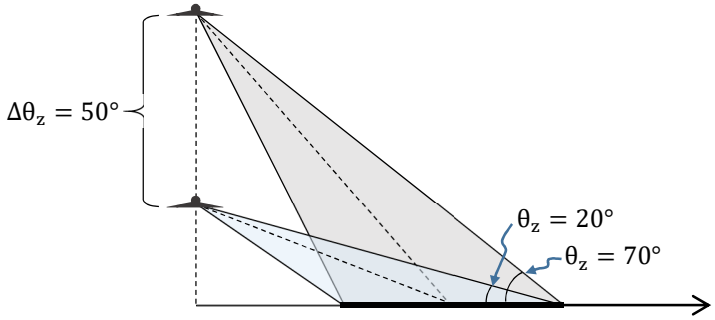

Fig 5. *CSAR Acquisitions undertaken at multiple heights. 32 measurement collections were completed over the elevation angle range of ≈50°.*

Each measurement collection was composed of 263,575 azimuthal measurement samples, for each polarisation, this being the number of times a transmitted pulse was sent into the scene and received by the aircraft. Each measurement pulse was transmitted from 200-1388 MHz, achieving a bandwidth of 1188 MHz.

With this bandwidth Airbus was aiming to achieve a slant range resolution (δ_r) of 0.13m and a vertical elevation resolution (δ_{er}) of 0.14m, calculated using equations (2) and (3) as follows,

$$\delta_r = \frac{c}{2F_{BW}} \tag{2}$$

$$\delta_{er} = \frac{\lambda_c}{2\Delta\theta_z} \tag{3}$$

Where $\Delta\theta_z$ is the change in elevation angle, as shown in Fig 5, and λ_c is the centre wavelength of the transmitted pulse.

Only the first circular measurement at the shallowest elevation angle of 18.29° elevation angle and a linear SAR collection conducted at the same altitude have currently been delivered to the authors at Cranfield's AGBSAR laboratory for analysis. However, there is still a great deal of information from these two acquisitions that can be used.

The data is provided in Airbus' standard Compensated Phase History Data (CPHD) format, which should not to be confused with other Complex Phase History Data (CPHD) formats used within the industry, e.g. National Geospatial Intelligence Agencies own data formats of the same name [11]. The main difference is that data provided by Airbus has already been motion compensated.

The authors' initial aim is to develop techniques from these first two datasets, and then extend these to the complete three-dimensional dataset, i.e. all elevations that were measured above the target area. The circular trajectory for the dataset delivered was provided in Earth Centre Earth Fixed (ECEF) reference frame [12]. To aid in the analysis of the collection trajectory, the ECEF reference frame was converted to North East Down (NED) local coordinate frame as follows,

$$\mathbf{P}_{NED} = R^T(\mathbf{P}_{ECEF} - \mathbf{P}_{Ref}) \tag{4}$$

Where:

$$R = \begin{bmatrix} -\sin(\phi)\cos(\lambda) & -\sin(\lambda) & -\cos(\phi)\cos(\lambda) \\ -\sin(\phi)\sin(\lambda) & \cos(\lambda) & -\cos(\phi)\sin(\lambda) \\ \cos(\phi) & 0 & -\sin(\phi) \end{bmatrix} \tag{5}$$

where λ and ϕ are the longitude and latitude respectively. The reference ECEF coordinate ($\mathbf{P}_{Ref}$) used in the transformation was set to the location of the lodge, measured accurately by Airbus during the trials to seven significant figures. The end result is shown in Fig 6.

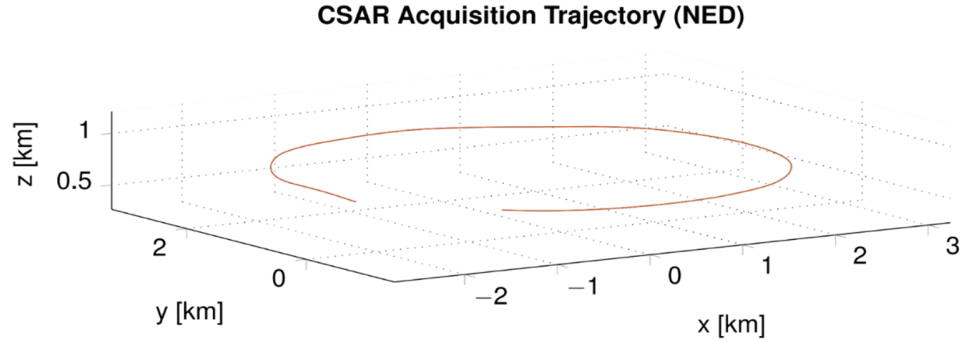

Fig 6. *CSAR acquisition trajectory for one of the 32 measurement collections conducted by Airbus over the Scandinavian lodge style target located at the Country Retreat Lodges holiday site in Mablethorpe, Lincolnshire. The collection was conducted at 18.29° elevation angle above image scene. Local coordinate frame, North East Down (NED) is used here to provide an easier reference frame to visualise the trajectory.*

4 DIFFICULTIES OF OPERATING AT LOW RADIO FREQUENCIES

The operating frequency range that the Bright Sapphire II instrument transmits over creates a number of challenges for a user trying exploit the collected data. The bandwidth desired is already heavily congested with other radio frequency transmissions from NATO to the Civil Aviation Authority, see Fig 7a.

Therefore, for the LF-SAR collection trials to go ahead, negotiations with Ofcom regulators and the MOD were undertaken, leading to the transmitted pulse containing null values (no transmission) at the frequency ranges defined by several Ofcom regulations, as shown in Fig 7b, where blue represents which frequencies can legally be transmitted.

The nulled frequency bands need to be accounted for before any image processing of the data can be undertaken. Fig 8b shows the effect that nulling has upon the raw compensated phase history data (CPHD), Fig 8a, and how it disrupts its continuity throughout the bandwidth. The nulled areas of phase data can detrimentally affect how the analyst can successfully use the data.

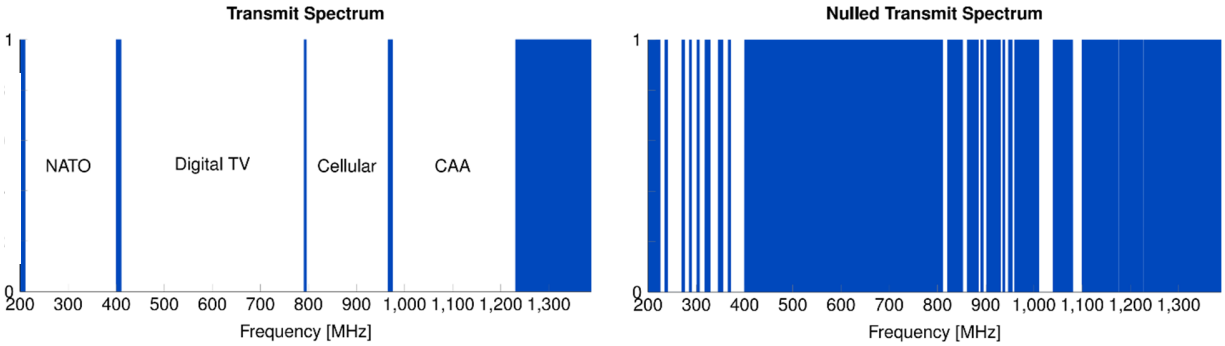

(a) **(b)**

Fig 7. *Transmitted spectrum investigation. Blue represents which frequencies can be legally transmitted over.*
(a) Visual representation of the congestion within the desired transmitted bandwidth.
(b) The actual transmitted bandwidth for the LF-SAR collection trials, as described in the Ofcom regulations agreed with Airbus.

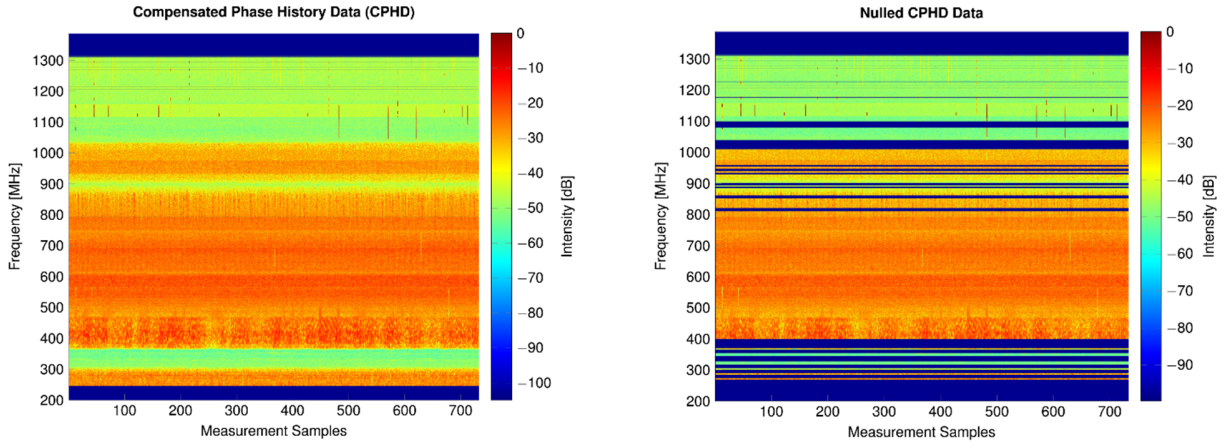

(a) **(b)**

Fig 8. *Compensated Phase History Data (CPHD) – Vertical Polarisation (VV). The raw phase data measured over the first 1° of the circular SAR data acquisition (the first 732 measurement samples).*
(a) The raw CPHD data as provided by Airbus, plotted in decibels [dB].
(b) The raw CPHD data shown in Fig 8a nulled, based on the data provided in the Fig 7b – The nulled transmit spectrum.

5 PRELIMINARY IMAGE PROCESSING

5.1 Identifying Radio Frequency Interferers

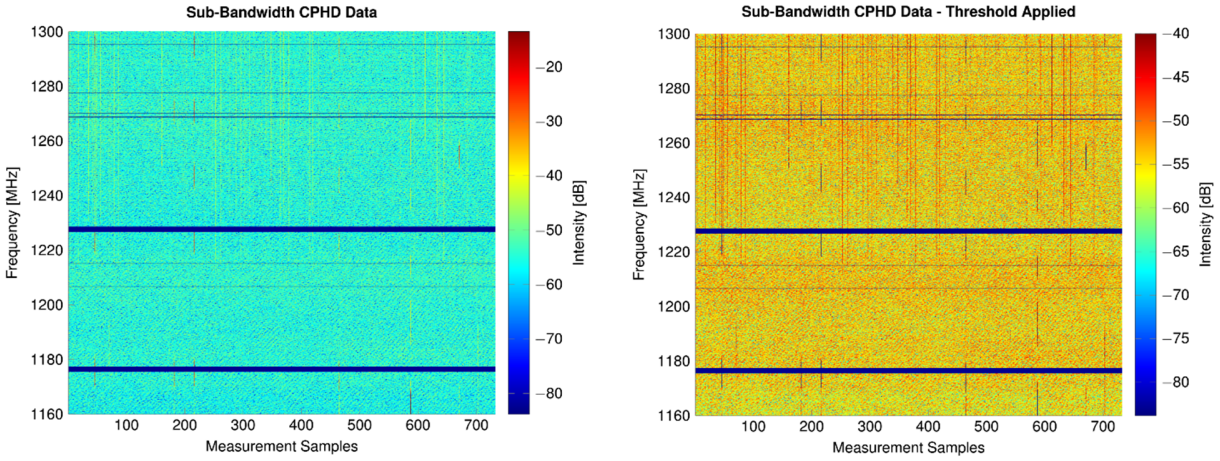

(a) **(b)**

Fig 9. *Sub-bandwidth CPHD data. Radio frequency interferers are clearly visible within the CPHD data, as vertical lines of high intensity.*
(a) Sectioned CPHD data.
(b) Intensity thresholding approach applied to the complex CPHD data in (a).

From a preliminary analysis of the phase history data it is clear that interference is going to be a significant challenge in producing the most exploitable SAR images from the LF dataset.

As described in Section 4 the inclusion of null frequency bands means that for any preliminary data analysis, a sub-bandwidth section of the phase history avoiding large null areas needs to be chosen first, to avoid unwanted effects with the preliminary formed images. Choosing higher frequency bands will also help reduce the effect of interference in the data, because as a general rule of thumb the higher the frequency band the *better* the image quality.

The following sub-bandwidth was chosen: 1160-1300 MHz. However, there is a side effect to reducing the bandwidth within the CPHD data, Airbus' initial range resolution can now no longer be achieved. The maximum range resolution for this sectioned CPHD data is now 1.07m, calculated using equation (2).

Fig 9a shows the same CPHD data from Fig 8b (i.e. vertical polarisation, VV) but with the sub-band section of data. Even with this bandwidth reduction, Fig 9a still shows signs of noticeable interferers. They are visible as vertical lines of high intensity scattered throughout the phase history data.

One simple filter method to help reduce the interference effects that will be carried forward to the imaging (time) domain is to apply a threshold determined by the absolute intensity of the complex phase history data.

The threshold works simply by investigating the absolute intensity of the data shown in Fig 9a (currently shown in decibels (dB)), and manually determining a cut-off intensity based on this result. For this data set, the cut-off intensity was 0.01, therefore when the thresholding is applied all absolute intensity values below this amount are set to 0. The result of this is shown in Fig 9b. It can be clearly seen there is now a lot more diversity in the range of absolute intensities within the data, shown by the significantly lower max intensity between Fig 9a and Fig 9b.

5.2 Linear Acquisition – Stripmap SAR Processing

As mentioned in section 3.3, a linear acquisition was collected over a 6km aperture, imaging a 6x0.5km area with the desired target lodge located centrally.

Using the SAR backprojection algorithm [14], [15] a stripmap SAR image can be formed of a 1x0.5km area about the targets location. Fig 10 shows a satellite image of the target area [13].

To show the effectiveness of the thresholding discussed in Section 5.1, Fig 11 and Fig 12 compare the effects without and with the thresholding applied to the CPHD data. The result between these two SAR images is a significant reduction in the interference.

Fig 10. *Satellite image of the measured target area. The complete image extent area is overlaid upon the figure. The NW corner of the target building is highlight and is located centrally in the image extent.*

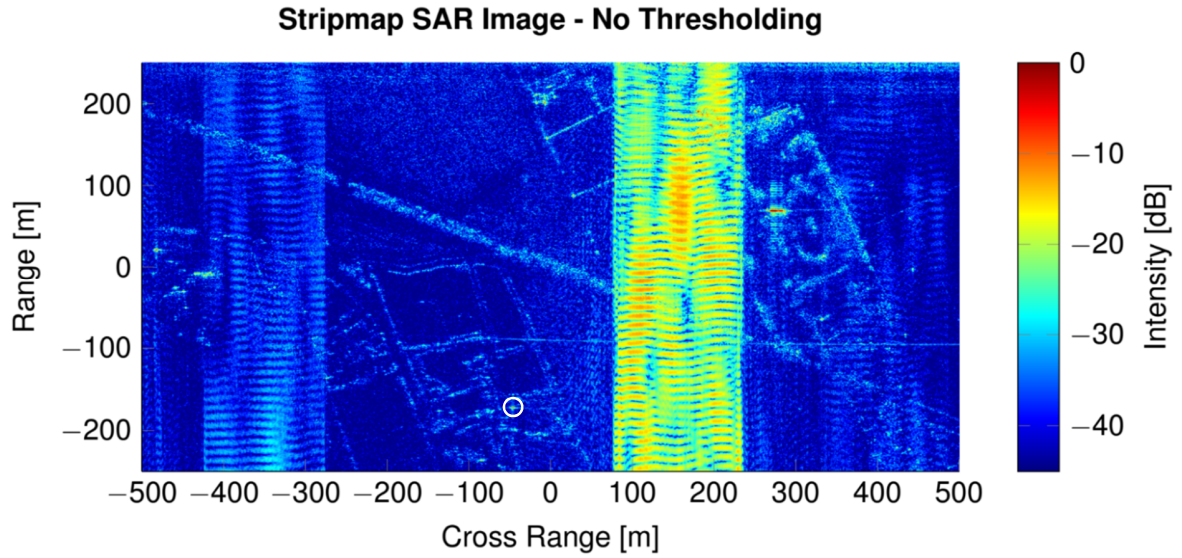

Fig 11. *Stripmap SAR image of the target area. No thresholding has been applied to the data, as a result RF interference has noticeably degraded the image quality. However, the large calibration sphere located within the building could still be identified and has been highlighted by the white circle plotted on the image.*

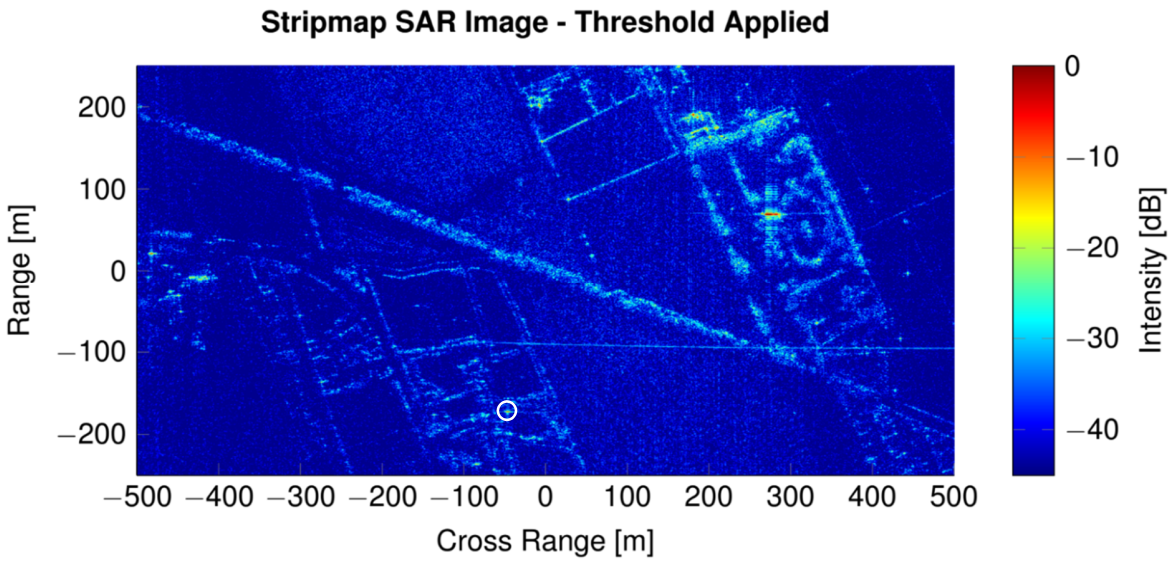

Fig 12. *Stripmap SAR image of the target area. Thresholding has been applied to the data, with a value of 0.01. As a result, RF interference has noticeably reduced, improving the image quality. The large calibration sphere located within the building has been identified and has been highlighted by the white circle plotted on the image.*

5.3 Circular Acquisition – CSAR Processing

Airborne CSAR image formation and processing can become a more involved challenge than the stripmap image processing showed previously. From a computational perspective, the CPHD data for the single circular acquisition delivered to the authors is approximately 64GB (263,575 measurement samples per polarisation), which represents a significant data processing challenge.

To aid in the computational task of processing such large datasets, the authors decided to split the data into separate *data-segments*. The data was split into 360 separate segments. This was done so that one can selectively form specific SAR images based on their desired angular location in the circular acquisition. This also allowed the authors to investigate a technique known as *multi-look* SAR imagery. Multi-look SAR is a process of producing SAR images of the same imaged area from different angular perspectives.

The multi-look technique can be useful when trying to determine the reflection/scattering characteristics of identified objects in the scene, as objects may appear at varying brightness's when imaged from different angular directions. The technique can also help reveal hidden objects that may only become bright when the radar is located at a certain angular position to the scene.

Fig 13 represents a set of 6 multi-look images of the target area. Each image is formed using 7320 measurement samples (therefore 10 data segments, of 732 measurement samples each). The lodge is located at approximately 0m in Range and 0m in Cross-Range. Target features can be seen to flash when illuminated from certain angles, and the effect of RFI is also variable. In total there were 36 images formed over the whole circular acquisition. For cross-reference a satellite image of area shown in the SAR images is shown in Fig 14 [13].

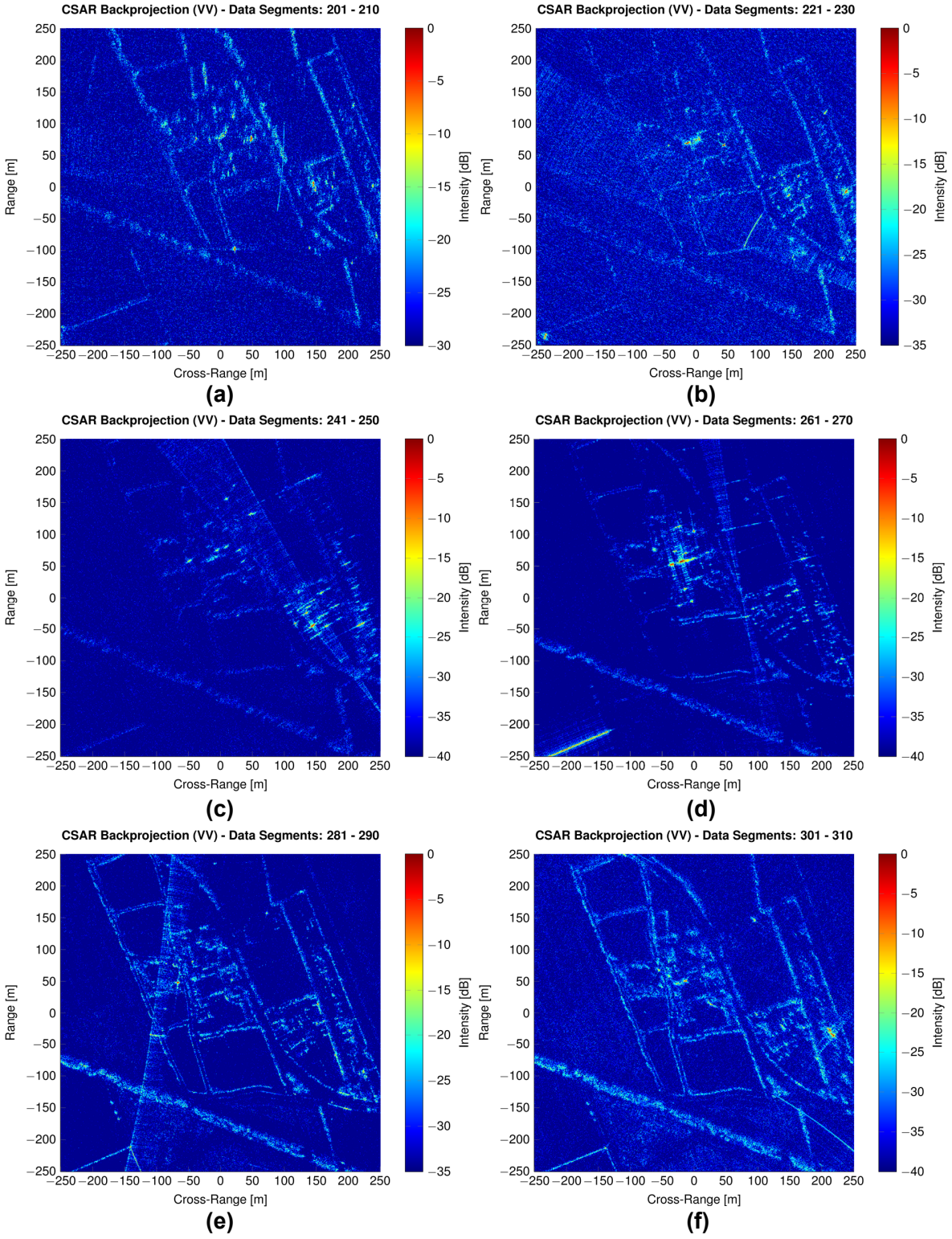

Fig 13. *Multi-look CSAR images formed using the backprojection algorithm. The whole circular acquisition was divided into 360 data segments, each with 732 measurement samples. 10 data segments were used to form each of the sub images shown. Target features can be seen to flash when illuminated from certain angles, and the effect of RFI is also variable.*

Fig 14. *Satellite image of the CSAR multi-look imaged area [13].*

7 CONCLUSION

A preliminary analysis of the airborne LF-SAR data-dome collection collected by Airbus Defence and Space Ltd has been presented. The authors have formed images of the two types of SAR acquisitions used during the collection: a linear stripmap SAR collection and a circular SAR acquisition.

The preliminary investigation of the compensated phase history data (CPHD) has shown that when operating SAR at low frequencies, interference has a substantial detrimental effect upon the quality of the CPHD data. To help reduce this effect the authors focussed primarily upon the top 150MHz of the transmitted bandwidth. The result is a collection of stripmap and CSAR multi-look images, formed using the backprojection algorithm which comprise a promising start to the analysis of this data.

In the next phase of the project, the authors plan to combine the multiple circular Airbus collections to form three-dimensional SAR images of buildings in the scene, revealing elements of building structure and contents.

ACKNOWLEDGMENTS

The authors would like to thank their collaborators at Airbus for providing the data and aiding in our preliminary work. We also thank our colleagues at DSTL for their continued interest in the work of the AGBSAR laboratory at Cranfield University, and for funding this project.

BIOGRAPHY

Brandon Corbett joined Cranfield University school of Defence and Security in October 2016 to begin his PhD within the field of Synthetic Aperture Radar (SAR), with a focus on image processing techniques and data analysis, with the aim of exploiting synthetic aperture radar signal processing to reveal concealed building features and phenomena.

Daniel Andre completed his PhD in Applied Mathematics / Theoretical Physics in 2000 at Bristol University. He has since conducted research in numerous Radar and SAR topics at DERA, QinetiQ, Dstl and now at Cranfield University, where he leads the Ground Based SAR Laboratory and teaches on various MSc courses.

REFERENCES

[1] B. Corbett, D. Andre, D. Muff, I. L. Morrow, and M. Finnis, "Imaging SAR Phenomenology of Concealed Vibrating Targets," in *12th European Conference on Synthetic Aperture Radar EUSAR.*, 2018, pp. 1–5.

[2] W. G. Carrara, R. S. Goodman, and R. M. Majewski, *Spotlight Synthetic Aperture Radar, Signal Processing Algorithms*, First. Artech House, INC, 1995.

[3] C. V. Jakowatz, D. E. Wahl, P. H. Eichel, D. C. Ghiglia, and P. A. Thompson, *Spotlight-Mode Synthetic Aperture Radar: A Signal Processing Approach*, First. Norwell, MA, USA: Kluwer Academic Publishers, 1999.

[4] J. Elgy, D. Andre, M. Finnis, and D. Blacknell, "Data Driven Corrections to Multistatic 3D Through-Wall Radar Imagery," in *Synthetic Aperture Sonar Synthetic Aperture Radar (SASSAR)*, 2018, vol. 40, pp. 199–208.

[5] R. Rudd, K. Craig, M. Ganley, and R. Hartless, "Building Materials and Propagation: Final Report," no. September, p. 123, 2014.

[6] ITU-R, "Effects of building materials and structures on radiowave propagation above about 100 MHz P Series Radiowave propagation," *Recomm. ITU-R P.2040*, vol. 1, 2013.

[7] ITU-R, "Propagation Data And Prediction Methods for the Planning of Indoor Radiocommunication systems and Radio Local Area networks in the Frequency Range 900 MHz to 100 GHz," 1999.

[8] M. Soumekh, *Synthetic Aperture Radar Signal Processing, with MATLAB Algorithms*, First. John Wiley & Sons, Inc, 1999.

[9] S. Doody, N. Hughes, E. Mak, D. Muff, and M. Nottingham, "Low Frequency Synthetic Aperture Radar Data-Dome Collection with the Bright Sapphire II Instrument," in *NATO SET 247 - Remote Intelligence of Building Interiors*, 2018, no. 1, pp. 1–10.

[10] D. Andre, K. Morrison, D. Blacknell, D. Muff, M. Nottingham, and C. Stevenson, "Very High Resolution Coherent Change Detection," *Radar Conf. (RadarCon), 2015 IEEE*, pp. 634–639, 2015.

[11] "Reading & Writing Sensor Independent XML (2.1)," Washington DC, USA, 2016.

[12] D. Koks, "Using Rotations to Build Aerospace Coordinate Systems," Edinburgh, Australia, 2008.

[13] Google, "Google Earth Pro." Google, Mountain View, CA, USA, 2018.

[14] D. C. Munson, J. D. O'Brien, and W. Kenneth Jenkins, "A Tomographic Formulation of Spotlight-Mode Synthetic Aperture Radar," *Proc. IEEE*, vol. 71, no. 8, pp. 917–925, 1983.

[15] M. D. Desai and W. Kenneth Jenkins, "Convolution Backprojection Image Reconstruction for Spotlight Mode Synthetic Aperture Radar," *IEEE Trans. Image Process.*, vol. 1, no. 4, pp. 505–517, 1992.